

The Board of Trustees  
of the Leland Stanford, Jr. University  
Center for Materials Research  
Stanford, California 94305-4045

Final  
IN-01-02  
58227  
p. 31

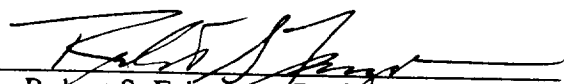
Final Technical Report  
on

## PROTEIN CRYSTAL GROWTH IN LOW GRAVITY

NASA-NAG 8-920  
CMR-94-4  
SPO #10544  
June 1, 1992 through May 31, 1994

Submitted to  
George C. Marshall Space Flight Center  
ES-76, Space Sciences Laboratory  
MSFC, AL 35812

Principal Investigator:

  
Robert S. Feigelson, Professor (Research)  
Center for Materials Research  
Stanford, California 94305-4045  
N95-13202 415) 723-4007

(NASA-CR-196980) PROTEIN CRYSTAL  
GROWTH IN LOW GRAVITY Final  
Technical Report, 1 Jun. 1992 - 31  
May 1994 (Stanford Univ.) 31 p

Unclass

## TABLE OF CONTENTS

ABSTRACT .....	1
INTRODUCTION .....	2
Effect of Growth Rate on Protein Crystal Quality .....	2
Control of Nucleation and Growth.....	5
CURRENT RESEARCH .....	9
Atomic Force Microscope Studies of Lysozyme Crystals .....	9
Thermonucleator Design .....	18
SUMMARY .....	27
REFERENCES .....	29

## **ABSTRACT**

This report details the research done under NASA Grant NAG8-920. This one year grant was extended over a two year period due to staffing changes. This research involved 1) using the Atomic Force Microscope (AFM) in a study on the growth of lysozyme crystals and 2) refinement of the design of the Thermonucleator which controls the supersaturation required for the nucleation and growth of protein crystals separately.

AFM studies of the (110) tetragonal face confirmed that lysozyme crystals grow by step propagation. There appears to be very little step pile up in the growth regimes which we studied. The step height was measured at  $\approx 54\text{\AA}$  which was equal to the (110) interplane spacing. The AFM images showed areas of step retardation and the formation of pits. These defects ranged in size from 0.1 to 0.4 $\mu$ . The source of these defects was not determined.

The redesign of the Thermonucleator produced an instrument based on thermoelectric technology which is both easier to use and more amenable to use in a  $\mu\text{g}$  environment. The use of thermoelectric technology resulted in a considerable size reduction which will allow for the design of a multi-unit growth apparatus. The performance of the new apparatus was demonstrated to be the same as the original design.

## **INTRODUCTION**

The goals of the research program funded by NASA Grant NAG8-920 were to use Atomic Force Microscopy to study the crystal growth and defect formation mechanisms during protein crystallization, and to refine the design of the Thernonucleator crystallization apparatus to make it more amenable to use in the laboratory and in  $\mu$ g.

The ultimate goal of the study of the crystallization of biological macromolecules is to produce high quality crystals for structural studies. In order to achieve this goal, the mechanisms of both growth and defect formation and their relationship to the crystal growth conditions must be understood and, based on this knowledge, methods developed to control the growth process to ensure the growth of useful crystals. The AFM studies described below addressed were directed at gaining an understanding of the growth process. The refinement of the Thernonucleator continued the development of an apparatus aimed at increasing crystal perfection during protein crystallization.

The research done under NAG8-920 was a outgrowth of our previous studies in this area. Our studies of isocitrate lyase established a relationship between growth rate and morphological perfection. The research on temperature induced nucleation and growth established a means of controlling the two phases of crystallization. Our initial research in these areas is described below.

### **EFFECT OF GROWTH RATE ON PROTEIN CRYSTAL QUALITY**

We initiated a study of isocitrate lyase (ICL) to learn what growth mechanisms led to the improved crystal quality and x-ray properties of the crystals grown in low gravity shuttle experiments. We first grew ICL crystals by the hanging drop method which duplicated the original work at DuPont Merck and yielded dendrite like morphologies. Next a vapor equilibrium cell was constructed with the idea of improving the viewing capability for flow visualization experiments in the expectation that a reduction in gravity driven flow might be responsible for the improvement in crystal quality. The cell volume was 20  $\mu$ l with a cross section of 3mm x 1mm giving a surface area for equilibration which was 1/3 of that of the hanging drops. Surprisingly, the crystals grown in this cell were not dendritic but had an equiaxed morphology similar to the space grown crystals (Fig. 1).

Growth experiments were also conducted in 1.88mm diameter capillary tubes using the vapor diffusion method. These experiments produced crystals with two different morphologies (Fig. 2). A total of four different crystal morphologies were observed in our laboratory. The predominant morphology observed has a cross section that appears to be a flattened "octagon". The ends of the "octagon" terminate in either a flat face or a wedge shape. This morphology is consistent with the orthorhombic symmetry of the isocitrate lyase unit cell

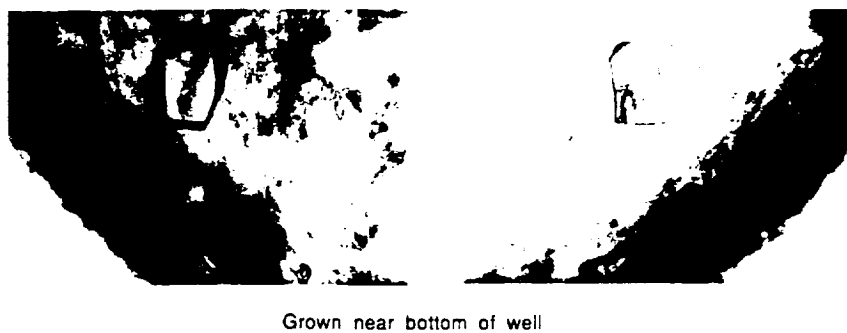
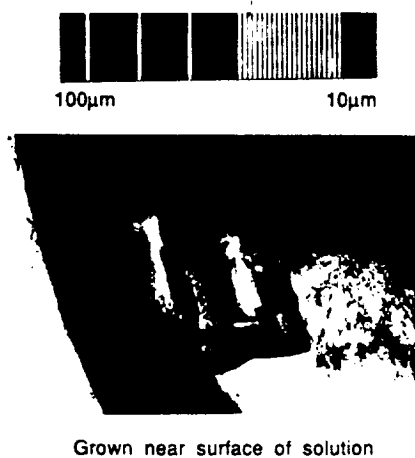


Fig. 1. Isocitrate lyase crystals grown in double well cell.



Fig. 2. Octagonal-like isocitrate lyase crystals grown in capillaries.

$b=123.1\text{\AA}$  and  $c=183.4\text{\AA}$ ) [1] with slow growing faces bounded by low index planes. A variation of this morphology was found in the crystals with the enhanced corner growth. The instability in growth occurred at the corners of the terminal faces of the "octagonal" form. X-ray diffraction studies of these "octagonal" crystals showed that they belonged to the same space group and had the same unit cell parameters as previously grown crystals.

The third morphology which was found were thin platelets of about  $5\mu$  thickness. These platelets were four sided with apex angles of  $82.5 \pm 1^\circ$  and  $98.1 \pm 0.5^\circ$ . This morphology is not readily explained by the orthorhombic symmetry and low index slow growth planes. The final morphology observed was the equiaxed crystals previously mentioned.

Preliminary results showed that the morphologies of the isocitrate lyase crystals grown under the conditions described above were not due to the sedimentation effect. Morphological stability and form seemed to be related to the rate of equilibration of the protein solution and the overall crystal growth rate. The solubility curve of ICL is not known, but the rate of supersaturation will be related to the rate of evaporation of the solution. The rate of evaporation of hanging drops and solutions in capillaries can be estimated by using the models developed by Fowles et al. [2] and by Sibille et al. [3,4]. Applying these models to ICL it was estimated that the rate of evaporation decreases by a factor of 5 when increasing drop size from  $4\mu\text{l}$  (terrestrial experiments) to  $30\mu\text{l}$  (space experiments). The change was more dramatic when comparing drops and capillaries (1.88mm dia.) of the same volume. The rate in the capillaries was 100 times slower. This was a strong indication that at least part of the improvement seen in the crystals grown in our laboratory was due to the rate of evaporation and hence the rate of supersaturation of the crystallizing solution.

The work of Sibille et al. [4] also suggests that the rate of evaporation is slower in space due to the formation of a salt rich layer at the surface of the drop. To test the possible effect of this hypothesis as well as other effects associated with gravity, isocitrate lyase crystals were grown in three sets of capillaries of different diameters (1.88, 2.56, 3.43, 4.97 and 5.97mm) oriented with the capillaries horizontal, vertical with the liquid surface up and vertical with the liquid surface down. In the larger capillaries (4.97 and 5.97mm) that contained crystals, the crystals were dendritic indicating a high supersaturation resulting from rapid equilibrium. The smaller capillaries with the liquid surface down developed a layer of amorphous or microcrystalline material in the liquid at the interface. This indicated that a layer of supersaturated (denser) solution was formed at the interface and held there by gravity. A platelet crystal did form in the 2.56mm tube and developed into a "blocky" crystal of poor morphology. Some small crystals also formed at the interface in the 1.88mm capillary. In the capillaries with the liquid surface up, gravity is expected to mix the denser surface layer with the bulk solution causing a slow change in supersaturation

throughout the liquid. A single, equiaxed crystal was formed at the bottom of the 1.88mm capillary which is consistent with a slower vapor equilibration rate leading to a slower growth rate.

Gravity should also cause fluid motion in the horizontal capillaries, but the mixing would be expected to be somewhat different. The pattern of crystallization in both the 1.88 and 2.56 horizontal capillaries showed small, needle like (perhaps "octagonal") crystallites mainly on the downward side of the tube. Again the equilibration was slow, but gravity moved the supersaturated solution from the interface to the lower wall and mixing was not as thorough as in the vertical capillaries.

## CONTROL OF NUCLEATION AND GROWTH

Non-seeded crystal growth is a two step process of nucleation followed by growth. The driving force (supersaturation) necessary for nucleation is much greater than that necessary for steady state growth and can lead to secondary nucleation and/or unstable growth. Our goal was to separately control these two phases of crystal growth in protein solutions.

Preliminary nucleation experiments using localized supersaturation (cooling) control were successful and have led to the design of the first prototype space flight hardware (The Thermonucleator). This design incorporated a more sophisticated localized temperature gradient control as well as a means of controlling the ambient temperature around the growth cell as an aid to localizing the nucleation as well as a means of controlling subsequent growth. (Fig. 3). With a cold spot temperature of 15°C and an ambient temperature of 25°C, the vertical temperature gradient above the cold spot was about 200°C/cm. The initial prototype apparatus is much larger than would be desirable for an actual flight experiment, but this allows for ease of modification to the growth cell and optical systems

The Thermonucleator was tested with water, Rochelle salt, lysozyme, horse serum albumin and  $\alpha$ -chymotrypsinogen A. In some of the tests the ambient temperature was changed to increase the growth rate. Ice crystals were readily grown from water and their size could be manipulated by adjusting the cold spot temperature.

Rochelle salt was grown from a solution saturated at 24°C. The experiment was begun with the ambient temperature set at 24°C and the cold spot at 16°C. In approximately two hours a crystal was visible. After 8 min, the crystal had grown to approximately 1mm in length. Lowering the ambient temperature to 20°C over a period of 4 hours (spot temperature was adjusted to match the ambient value after nucleation had occurred) produced a crystal which measured 3.3mm x 2.0mm.

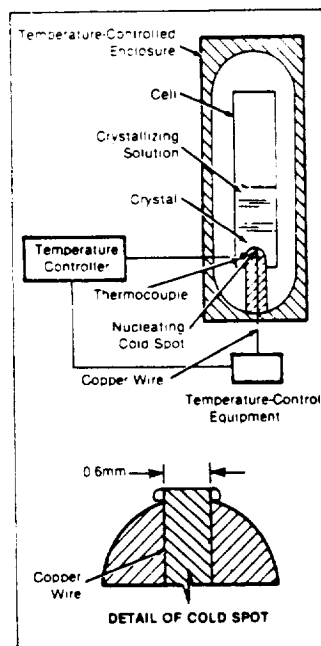
The first protein studied was lysozyme which has a solubility that increases with temperature. A saturated solution at 25°C was prepared using Pusey's solubility data [5]. The enclosure temperature was 25°C and the cold spot 15°C. The first crystals appeared in 4.5 hrs;

## Thermonucleator

Localized cooling causes localized supersaturation and hence localized nucleation.  
Marshall Space Flight Center, Alabama

The thermonucleator (see figure 1) is an apparatus that controls nucleation in a selected region of a crystallizing solution by varying the local temperature and thus the local supersaturation. This apparatus potentially offers better control of the crystallization process in an aqueous solution than does the use of a stream of cold gas to induce nucleation by cooling part of the bottom of a crucible that contains a hot solution. The ability of the thermonucleator to nucleate crystals in a small spot has been demonstrated with water, Rochelle salt, and lysozyme. The latter example represents the first application of active control of nucleation to the growth of crystals of biological macromolecules. One future modification of the thermonucleator could be the addition of a nucleation-detection subsystem that would switch the apparatus from the nucleation mode to the growth mode.

The thermonucleator includes a chamber that controls the ambient temperature of the cell that contains the solution from which crystals are to be formed. The temperature of a small spot near the bottom of the cell can be controlled independently of the ambient temperature. This small spot is the end of a 0.6-mm copper wire (other sizes and materials can be used). The wire is at-



The Thermonucleator controls nucleation in a selected region of a crystallizing solution by varying the local temperature and, hence, the local supersaturation.

tached to a larger copper rod that dips into a Dewar flask that contains liquid nitrogen. The temperature of the small spot is controlled by use of a heater attached to the copper rod. Feedback is provided by a thermocouple and a temperature controller.

Local supersaturation and nucleation could also be induced and controlled by other techniques. For example, in the case of crystallization of biological macromolecules, the temperature-controlled wire could be replaced by a small source of precipitating agent to induce nucleation. Alternatively, the temperature-controlled wire could be replaced by an electrode, and electric current or the electric field between this electrode and another could be used to induce nucleation. Neither of these two concepts has yet been reduced to practice.

This work was done by Robert C. DeMattei and Robert S. Feigelson of Stanford University for Marshall Space Flight Center. For further information, write in 101 on the TSP Request Card.

Inquiries concerning rights for the commercial use of this invention should be addressed to the Patent Counsel, Marshall Space Flight Center [see page 22]. Refer to MFS-26212.

Fig. 3. Schematic of Thermonucleator showing growth cell, cold spot, cold spot temperature control, and ambient temperature control and article taken from NASA Tech Briefs, October 1993, pg 62.

ORIGINAL PAGE IS  
OF POOR QUALITY



a somewhat longer incubation time than that for the Rochelle salt. The growth rate of lysozyme was much slower than Rochelle salt. Lowering the temperature increased the growth rate, but led to a polycrystalline cluster lying exactly on the surface of the cold finger.

In an effort to limit the number of lysozyme crystals which grew, crystals were nucleated and allowed to grow for a period of time. Then the temperature was raised and all but a few of allowed to dissolve. The remaining crystals were allowed to regrow at lower supersaturation. During this growth sequence, one large (270 $\mu$ ) crystal and several smaller crystals were formed on the cold finger.

In the case of materials exhibiting retrograde solubility (solubility decreases with temperature), the nucleating probe would have to be kept warmer than the surrounding solution and therefore significant thermal convection would be expected. To determine whether strong convection would a) prevent nucleation, b) cause nuclei to form away from the probe, c) cause the nuclei which form on the probe to move away from the probe tip and/or d) effect nucleation density, two proteins which have retrograde solubility were studied: 1) horse serum albumin (HSA) (MW  $\approx$  60,000) and 2) bovine pancreas  $\alpha$ -chymotrypsinogen A (aCA) (MW  $\approx$  26,000). In addition, these two proteins have another characteristic in common, while they are known to have retrograde solubility, [6,7] their actual solubility-temperature relationships in solution are not well characterized. The latter provided an excellent opportunity to study the ability of the Thermonucleator to produce, within a short period of time, controlled crystallization in the absence of phase equilibria information.

The general approach used to nucleate these proteins without the benefit of knowing their solubility behavior was to prepare a near saturated to slightly supersaturated solution based on the known crystallization procedures [8, 9] and to slowly raise the probe temperature until nucleation occurred. The ambient temperature was also increased to raise the saturation of the bulk of the solution.

The selected "retrograde" proteins (HSA and aCA) were successfully nucleated using the Thermonucleation technique. The horse serum albumin crystals were nucleated on the probe at a temperature of 29°C, with the ambient temperature set at 16°C. The HSA crystal was approximately 20 $\mu$  at the widest point and was the largest crystal of this material observed in this series of experiments. The  $\alpha$ -chymotrypsinogen A crystals were nucleated at a probe temperature of 20°C with the ambient temperature set at 9°C. Figure 4a shows three aCA crystals at an early stage of growth (the largest crystal is about 27 $\mu$  along the base line). After a week of growth (Fig. 4b), the largest crystal was approximately 52 $\mu$ .

The actual nucleation and growth conditions for these crystals were not optimized, but represented a best estimate of the conditions based on the other growth techniques. [8,9] These results clearly demonstrated that the Thermonucleation technique can be applied to proteins whose

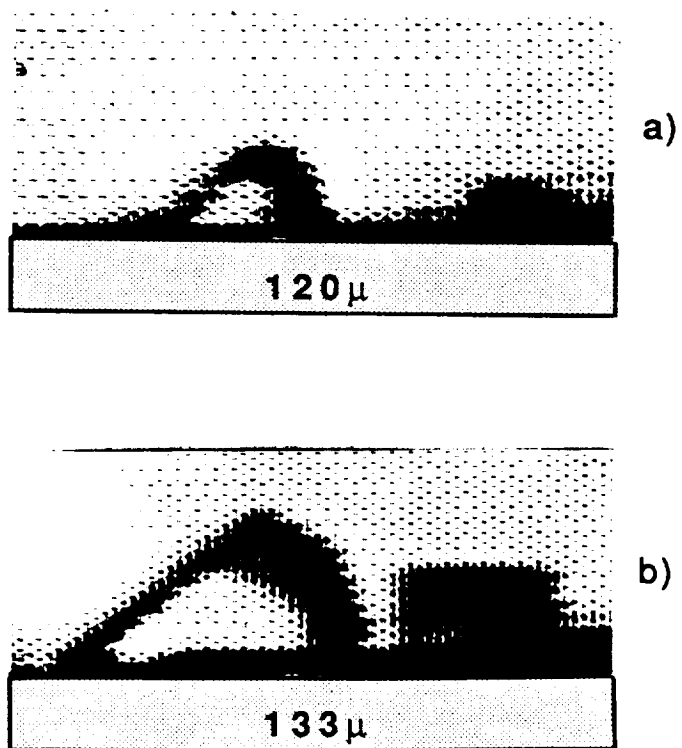


Fig. 4.  $\alpha$ -chymotrypsinogen A crystals nucleated in the Thermonucleator; a) shortly after appearance of the crystals, b) after one week of growth. Textured area shows location of a section of the temperature controlled probe. Photographed from a TV monitor.

solubility decreases with increasing temperature and to systems whose solubility behavior is known only in a general way (i.e., more crystals are formed if the temperature is lowered {raised})).

It has been suggested that the Thermonucleation technique could only be applied to solutions that were "sufficiently viscous to suppress convection to the extent necessary to prevent nucleation in undesired sites"[10]. The tendency of a solution to convect due to a temperature difference is given by the thermal Rayleigh number (Ra)

$$Ra = \frac{g c_p \rho^2 \beta L^3 \Delta T}{\mu k} \quad 1)$$

where  $g$  is the acceleration due to gravity,  $c_p$  the specific heat,  $\rho$  the density,  $\beta$  the thermal expansion coefficient,  $L$  the length (2cm),  $\Delta T$  the temperature difference (13°C),  $\mu$  the viscosity and  $k$  the thermal conductivity. Using equation 1 and the values for the material properties at 20°C, [11] Ra was calculated to be  $1.45 \times 10^6$ , which is well in excess of the critical Rayleigh number for the occurrence of natural fluid convection in these water solutions ( $\approx 300$  [12]). Strong flows were indeed observed by the movement of small particles in the growth cell. However, the results of the nucleation experiments indicated that crystals can be nucleated even in the presence of these flows.

## **CURRENT RESEARCH (NAG8-920)**

The current research was focused in two areas: First was the study of growth mechanisms and defect generation during protein crystallization. This study utilized the Atomic Force Microscope to investigate the surface of the crystals. Second was the redesign of the Thermonucleator to develop an instrument for general laboratory use and for use in  $\mu\text{g}$ . The results of these investigations are detailed below.

## **ATOMIC FORCE MICROSCOPE STUDIES OF LYSOZYME CRYSTALS**

Atomic Force Microscopy (AFM) was used to study the (110) surfaces of tetragonal lysozyme crystals. The objectives of this research was to study the growth mechanism(s) of macromolecular crystals and to image defects on the growing surface. The hen egg white lysozyme crystals were grown externally to the microscope and then transferred into the instrument under a slightly supersaturated solution to ensure continued slow growth during the AFM scans. Two different AFM's were used during this study; a Topometrix and a Digital Instruments Nanoscope III.

## EXPERIMENTAL

The lysozyme crystals were grown by the sitting drop method from lysozyme solutions that were buffered by 0.1M sodium acetate at pH 4.0. The well solution was 4% sodium chloride. A typical growth was done from a 100 $\mu$ l drop which consisted of 50 $\mu$ l of protein solution and 50 $\mu$ l of well solution. The lysozyme solubility at these end points were 37mg/ml (2% salt) and 3.5mg/ml (4% salt) [5]. Crystals were grown with initial lysozyme solution concentrations of 43, 30, 21 and 13mg/ml. The results are summarized in Table 1.

Table 1. Results of lysozyme crystal growth

Starting Conc.	Nucleation Time	Number of Crystals	Relative Size	Percent Good Crystals
43mg/ml	6 days	$\approx$ 500	0.1-0.75	20
30mg/ml	4 days	$\approx$ 100	$\approx$ 0.75	70
21mg/ml	15-25 days	8	0.2-1.5	100
13mg/ml	4 days	7		0-form not recognizable

Crystals for the AFM studies were grown on small substrates which were subsequently transferred to the liquid cell of the AFM. The crystals were stabilized by immersing them in a slightly supersaturated lysozyme solution. Suitable (110) surfaces were chosen using the optical microscope built into the AFM. The tip of the AFM was carefully lowered onto the crystal surface and the force adjusted to image the surface without causing noticeable damage.

## RESULTS

A large fraction of the effort devoted to the AFM study was expended in developing methods to image the crystals on the Topometrix apparatus since this machine was readily available. Unfortunately, this machine was not well suited for the research we wished to do. The optical viewing angle of 45° was less than ideal for selecting good crystal surfaces and for placing the tip accurately. Initial images obtained on this instrument indicated that, despite the use of slightly supersaturated lysozyme solutions in the cell, the crystals were dissolving. The dissolution was traced to the heating of the liquid cell by the electronics in the base of the instrument and by the lamp used for optical observation. Using an external lamp slowed, but did not eliminate the heating problem and temperatures in the cell reached as high as 35°C. Even if the solution could be supersaturated enough to stop the dissolution of the crystals, this temperature is well into the range where the orthorhombic and not the tetragonal phase of lysozyme is stable. Only a few images were obtained in this phase of the study.

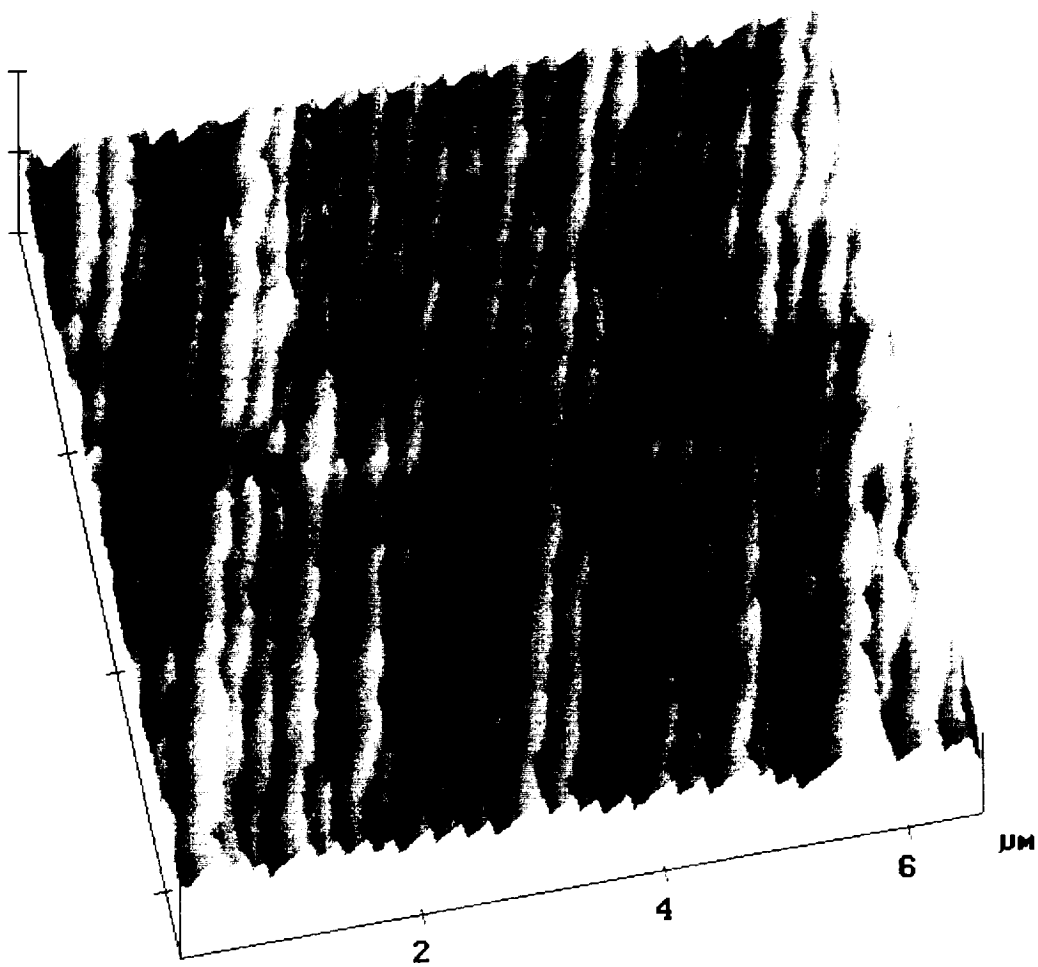


Fig. 5. AFM image of lysozyme crystal (110 face) showing layer growth with a defect at center of left hand edge.

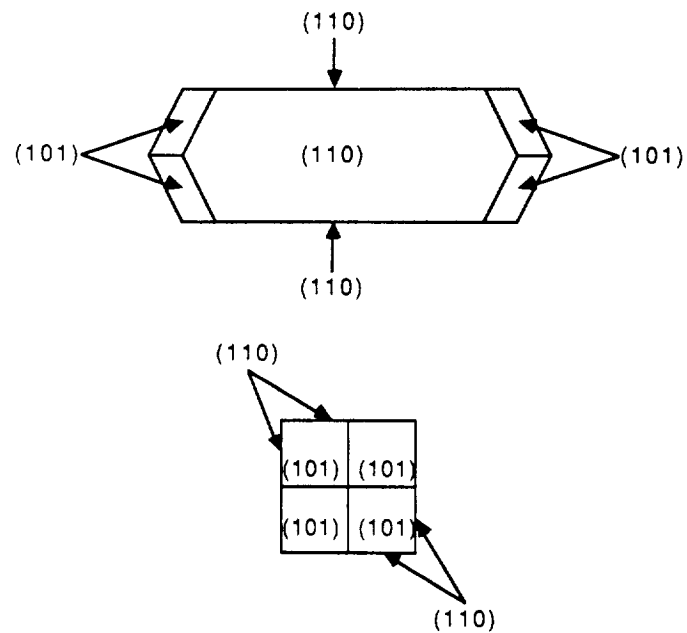


Fig. 6. Schematic of tetragonal lysozyme crystal.

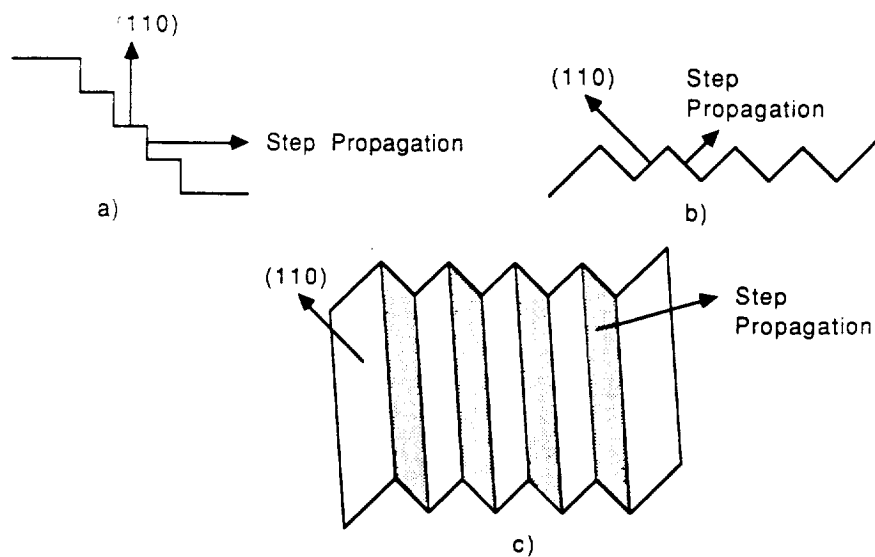


Fig. 7. Schematic showing step propagation on  $(110)$  face of tetragonal lysozyme. a) Edge view, b) edge view with crystal rotated and c) view with crystal rotated and tilted out of plane (similar to view in fig. 5)

A Digital Instruments Nanoscope III became available for a short period of time and the lysozyme studies were transferred to this unit. The vertical viewing arrangement made it much easier to select good crystal faces and to position the scanning tip accurately. This apparatus did not have a heating problem. Figure 5 shows a typical image of a (110) tetragonal face of a lysozyme crystal (fig. 6). This figure shows an almost periodic array of steps on the face (fig. 7). Because of the almost linear edges of these steps, it was assumed that the source of these steps was far from the field of view. It was obvious that the crystal grew by the generation and spread of ledges. The source of these ledges could be either a screw dislocation or two dimensional nucleation (both have been observed for lysozyme [13]). A defect appears near the middle of the left edge of the scan. A section of the ledges approximately 0.2 to 0.3  $\mu$  long lags behind the rest of the step. The cause of this localized slowing of the lateral spread of the steps was not obvious. However, the offset of the ledges indicated that the source of the steps was somewhere off the left edge of this scan and the steps spread from left to right.

Figure 8 is a magnified view of a surface similar to that shown in figure 5 but viewed at a lower angle. Here eight steps are distinctly visible over a range of 350 to 400  $\text{\AA}$  which yields a step height of 40 to 50  $\text{\AA}$ . This is seen more clearly in figure 9 which shows a line trace and analysis of a series of steps. The plateau areas of the steps are quite flat showing a rise of about  $1 \pm 0.5 \text{\AA}$  (the height measurement on second plateau from the right is slightly exaggerated due to the placement of the left indicator arrow). The step height based on the the analysis of the two steps at the left of the trace is 53.9  $\text{\AA}$  which compares to 55.9  $\text{\AA}$  calculated from the unit cell parameters. The double height step at the left is an example of step pile-up which can also be seen in the accompanying micrograph and has also been seen by Durbin [13].

Figure 10 shows a pit developing in the crystal. The apparent bottom of the pit measures 0.2  $\mu$  x 0.45  $\mu$  and lies approximately 200  $\text{\AA}$  below the uppermost layer shown. It is likely that this defect will continue to grow since the supersaturation decreases down the walls of the pit lowering the growth rate and preventing the pit from filling in. In the extreme case, this will lead to "hopper" growth.

## CONCLUSIONS

The AFM studies confirmed that lysozyme grows by a step growth mechanism. It is assumed that the steps spread by the attachment of molecules at the ledge sites. The predominate step height was  $\approx 54 \text{\AA}$  although some step bunching was observed. The source of the steps was not determined.

Large scale (0.1 to 0.4  $\mu$ ) defects were observed in growing lysozyme crystals. In one case, the defect took the form of a localized retardation of the step spreading rate. In another, a pit was formed on the growing face. The exact cause of the defects was not determined. These

defects do not represent the limit of observation by the AFM technique. In figure 10, an arm of  $\approx 200\text{\AA}$  width can easily be observed coming off the main pit and step heights of  $\approx 50\text{\AA}$  can be easily measured in other scans. This dimension scale approaches that of the unit cell dimensions for smaller proteins and the protein molecular dimensions for some larger proteins. With some care, defects involving a few molecules should be observable in protein systems.



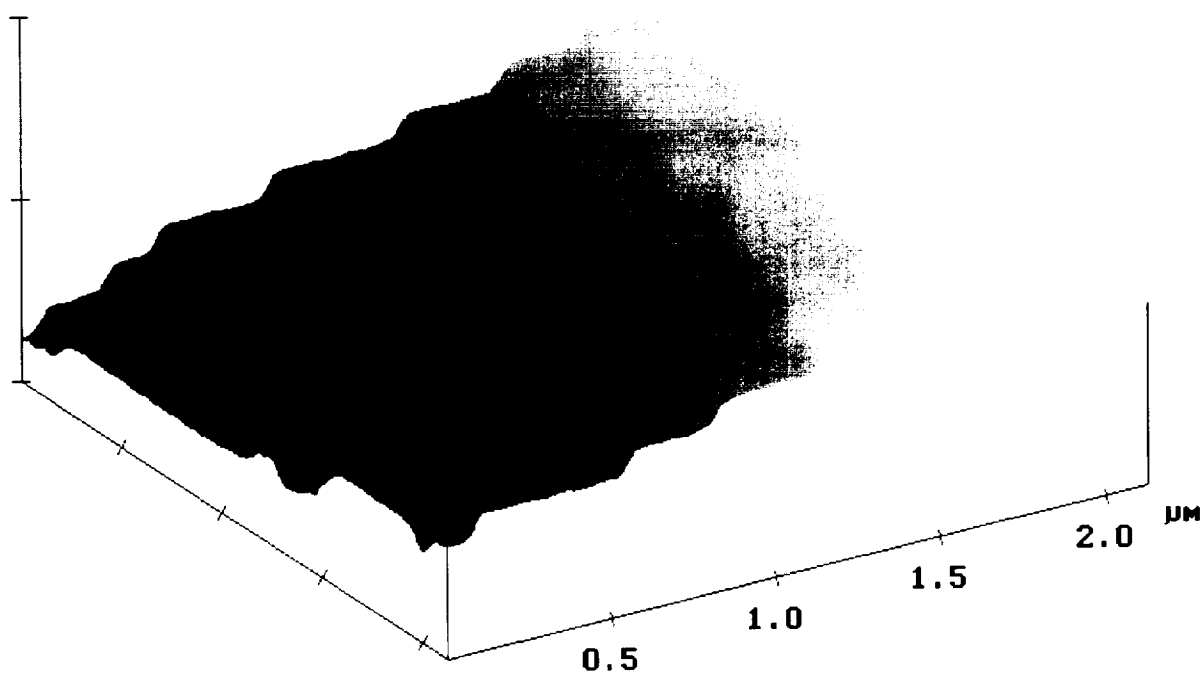


Fig. 8. Higher magnification, lower angle AFM image showing steps on surface.

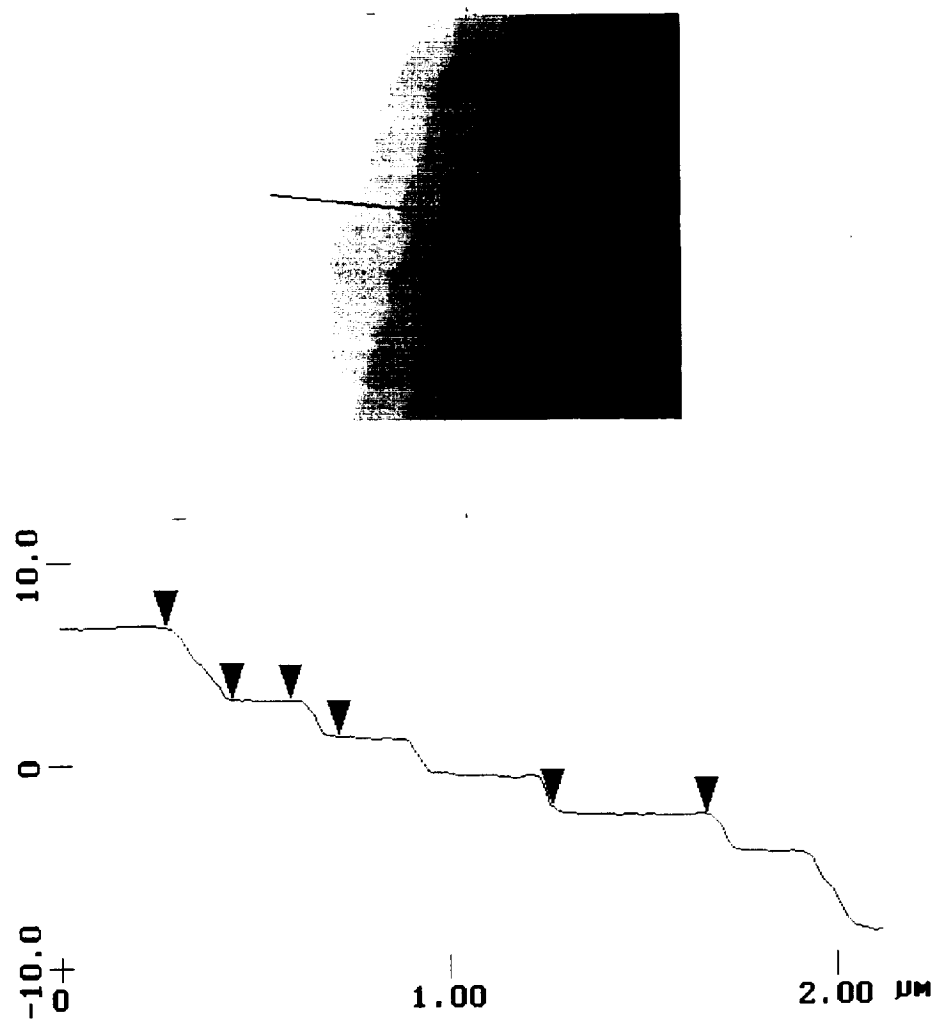


Fig. 9. Analysis of steps on lysozyme crystal. Note that left most step consists of two layers.

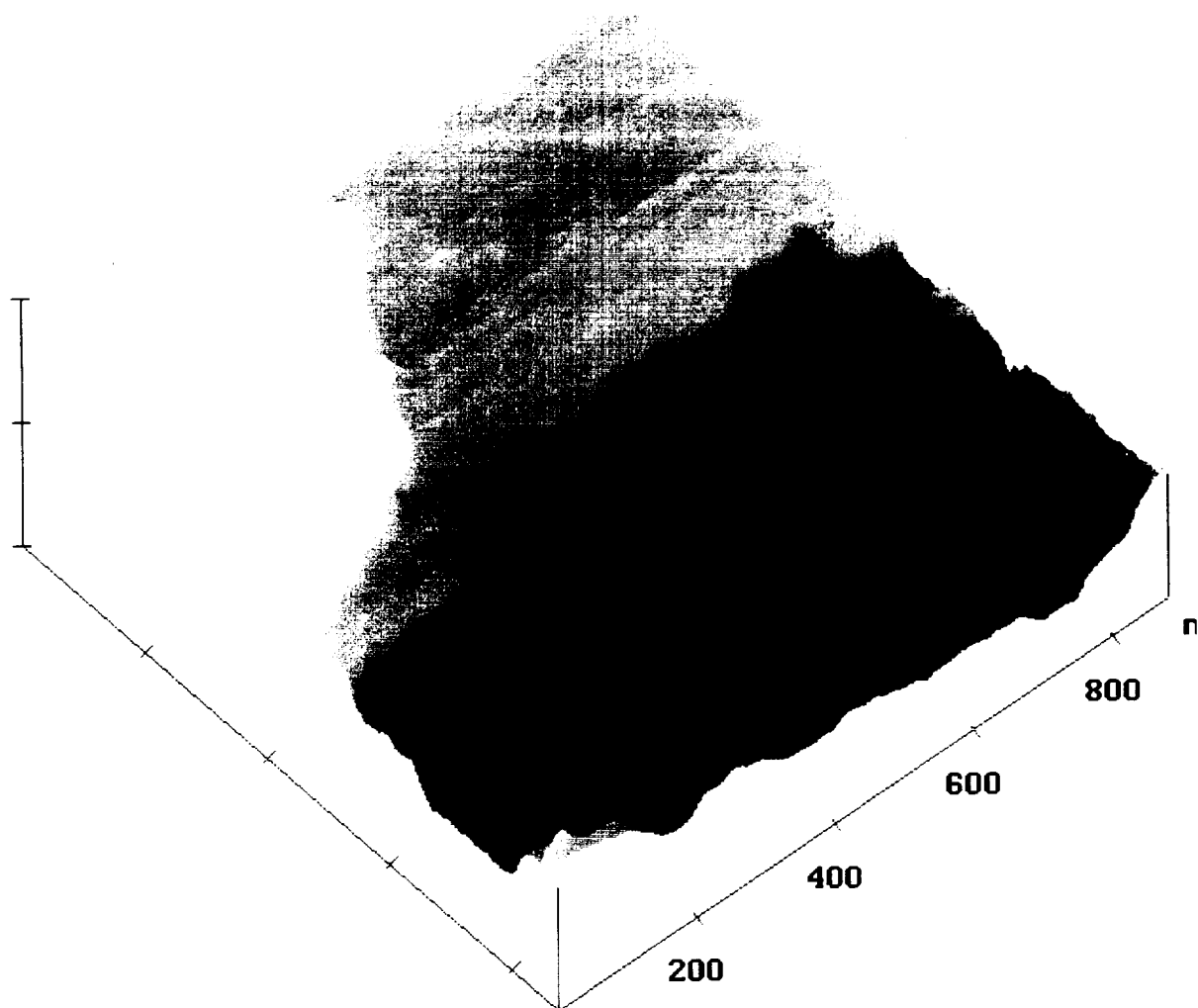


Fig. 10. AFM image of a pit forming on a  $110$  face of a lysozyme crystal.

## THERMONUCLEATOR REDESIGN

The original thermonucleator was developed to prove the concept of using temperature to separately control the nucleation and growth phases of the crystallization process. It was designed as a laboratory system that could be easily modified to test new ideas and the apparatus will still be used in this manner. However, the size of the thermonucleator and its temperature control systems were not well suited to either commercial applications or for use in a  $\mu\text{g}$  environment. The goal of this redesign was to produce an instrument that both was smaller and used temperature control methods which would be compatible with a  $\mu\text{g}$  environment. The new design must also allow observation of the growing crystal and the possibility of using other instrumentation techniques to measure the conditions around the growing crystal.

### DESIGN CRITERIA

The new design was built around the same size cell that was used in the original apparatus. This cell measures 0.5in. x 0.5in. x 1.75in. and is made of either fused quartz or plastic. Any final design must accommodate cells of smaller base dimensions for use with proteins that are available in limited amounts.

The most compact and easily controllable method of heating and cooling the apparatus was by means of thermoelectric elements. The thermoelectric units needed to be compact in order to keep the overall size of the thermonucleator within reasonable limits. The size criterion also dictated using fluid cooling of the thermoelectric elements rather than air cooling.

Finally, the design must incorporate adequate viewing ports so that the growing crystal can be observed by whatever means the investigator chooses. This dictated that there be windows on three sides of the cell and provision for back lighting on the fourth.

### THERMOELECTRIC COOLERS FOR AMBIENT TEMPERATURE CONTROL

The temperature of the air volume around the cell is controlled by two thermoelectric units placed at the top and bottom of the cell. The size of these units was dictated by the size of the thermoelectric elements. The elements selected measured 8mm x 8mm and had a wattage rating of 1.8 watts. Eight of these elements were placed in a square pattern (fig. 11) in each of the thermoelectric units for a total heat transfer capacity of 28.8 watts. The final dimension of each unit was 1.5in. x 1.5in. and the height of the temperature controlled volume was 1.125in. The side wall of this volume were made from 0.125in. plastic. Assuming a thermal conductivity for the walls of  $5.5 \text{ BTU} \times [\text{hr} \times \text{sq.ft.} \times (^\circ\text{F/in})]^{-1}$ , an inner temperature of  $4^\circ\text{C}$  and an outer temperature of  $25^\circ\text{C}$ , the heat flow into the volume around the cell was 22.8 watts. The thermoelectric units as designed were adequate to control the ambient temperature around the cell.

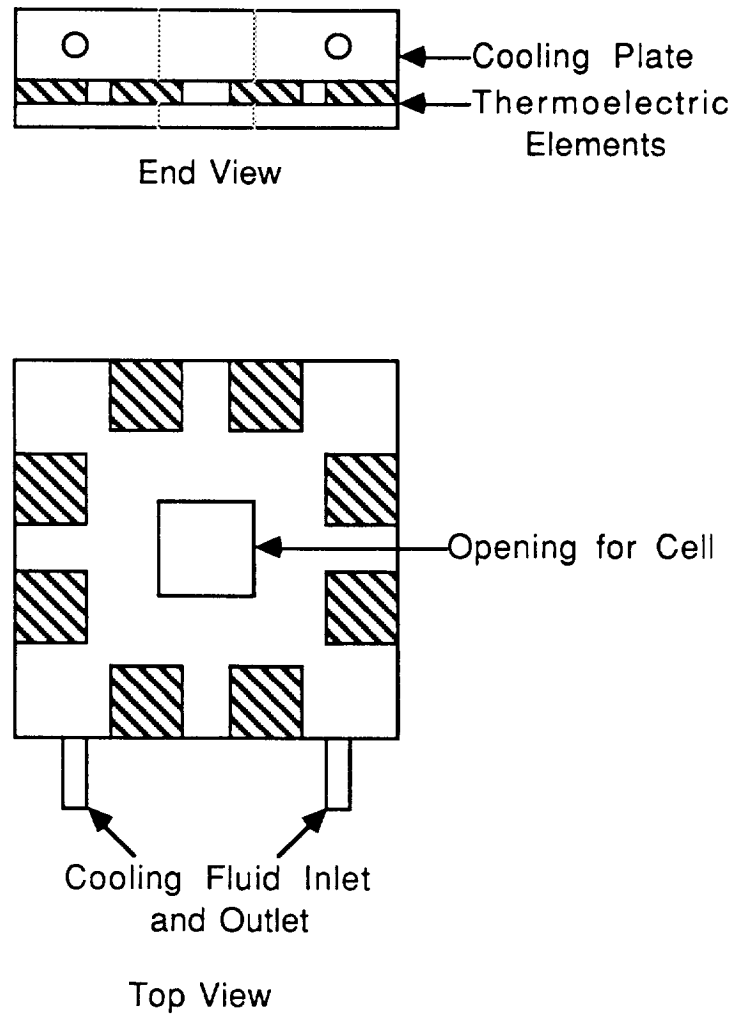


Fig. 11. Schematic of the ambient temperature control unit of the Thermonucleator.

## THERMOELECTRIC COOLER FOR NUCLEATION PROBE

The cooler for the nucleation probe was designed around a 4.5 watt thermoelectric element that measured 12mm x 12mm. This element was selected for size considerations. The element was connected to the nucleation probe by a tapered brass adaptor (fig. 12) This design appears to be adequate for the temperature range of 0°C to 35°C.

## OVERALL DESIGN

The outer dimensions of the thermonucleator were chosen to house the components previously described. Space was allowed for running the wiring and cooling water internally. Both the water connections and the electrical connection were brought out the rear of the apparatus using connectors that could be incorporated into a fixed rack if the thermonucleator was to be used in a working rather than a testing environment. The overall dimensions of the final design were 3in. x 3in. x 3.75 in.high. The apparatus is shown in figures 13 and 14.

## TEMPERATURE CONTROL

The ambient and spot temperatures were sensed with thermistors. The outputs of the thermistors were connected to two Alpha Omega Instruments Series 2 TC<sup>2</sup> thermoelectric element controllers. These were bipolar units which automatically switch the current polarity to provide heating and cooling as needed. This combination provided temperature stability to better than  $\pm 1^\circ\text{C}$  when measured by thermocouples placed on the tip adaptor and in the temperature controlled space around the cell.

## TESTING

The spot temperature was calibrated against the set point of the controller. Temperatures were measured both on the adaptor between the thermoelectric element and the cell, and on the spot itself. The results at an ambient temperature of 25°C is shown in figure 15.

The initial crystallizations were the growth of ice crystals from water. The ambient temperature was set at 10.3°C and the spot set point temperature was varied over a range of 6.3°C. The ice crystal was domed shaped following the freezing isotherm and varied in size from 0.24mm to 1.56mm (fig. 16).

Hen egg white lysozyme was used to test the new Thermonucleator's ability to crystallize proteins. The crystallizing solution contained 58mg/ml of lysozyme in a 0.1M sodium acetate buffer at pH 4.0 and 2% sodium chloride. This solution was slightly supersaturated at 25°C ( $[\text{concentration} - \text{solubility}]/\text{solubility} = 0.2$ ) [5]. The ambient temperature was set at 15°C and the spot temperature at 10°C which produced a local supersaturation of 3.0. After approximately 90 hours crystals appeared on the tip of the cold probe ( fig. 17a). The probe temperature was further lowered to -5°C raising the supersaturation to 6.0. In 2 hours, both secondary nucleation and rapid

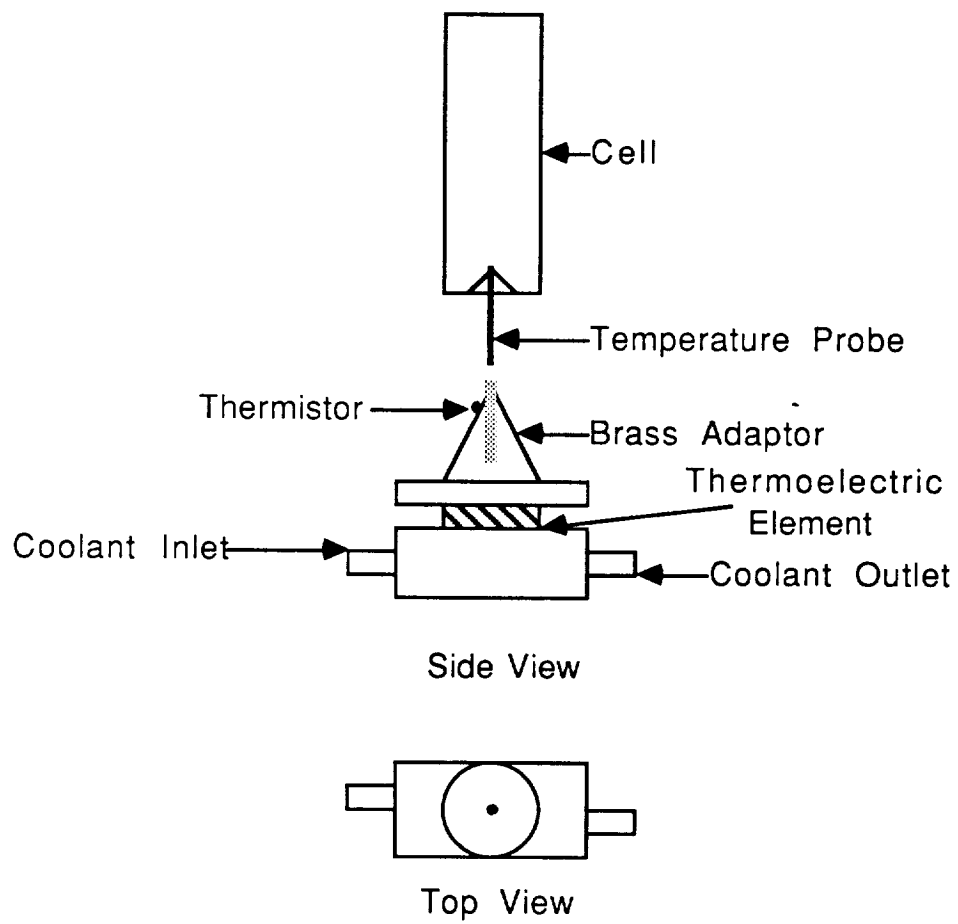


Fig. 12. Schematic of the spot temperature control unit.

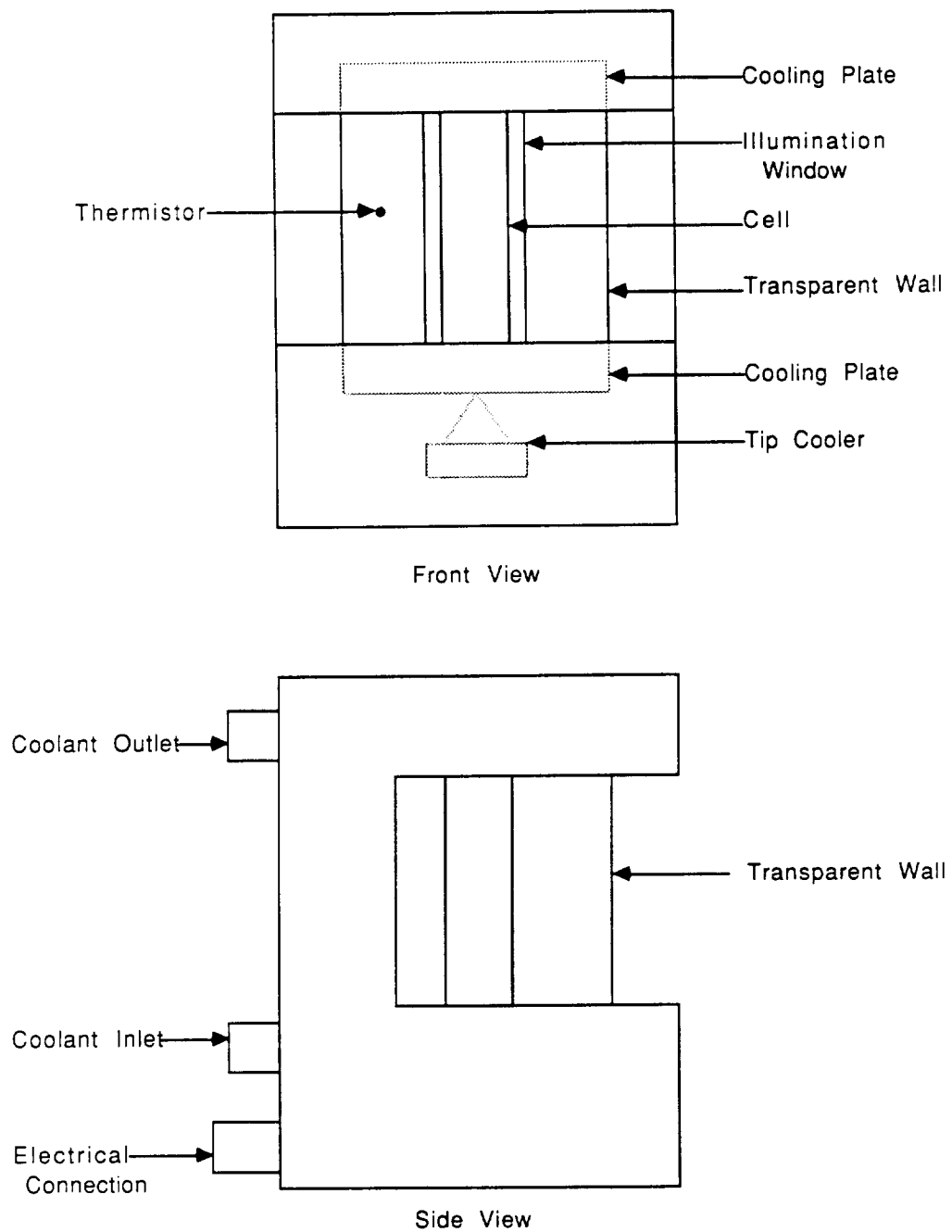


Fig. 13. Schematic of the Thermonucleator.





Fig. 14. Front and rear views of the Thermonucleator.

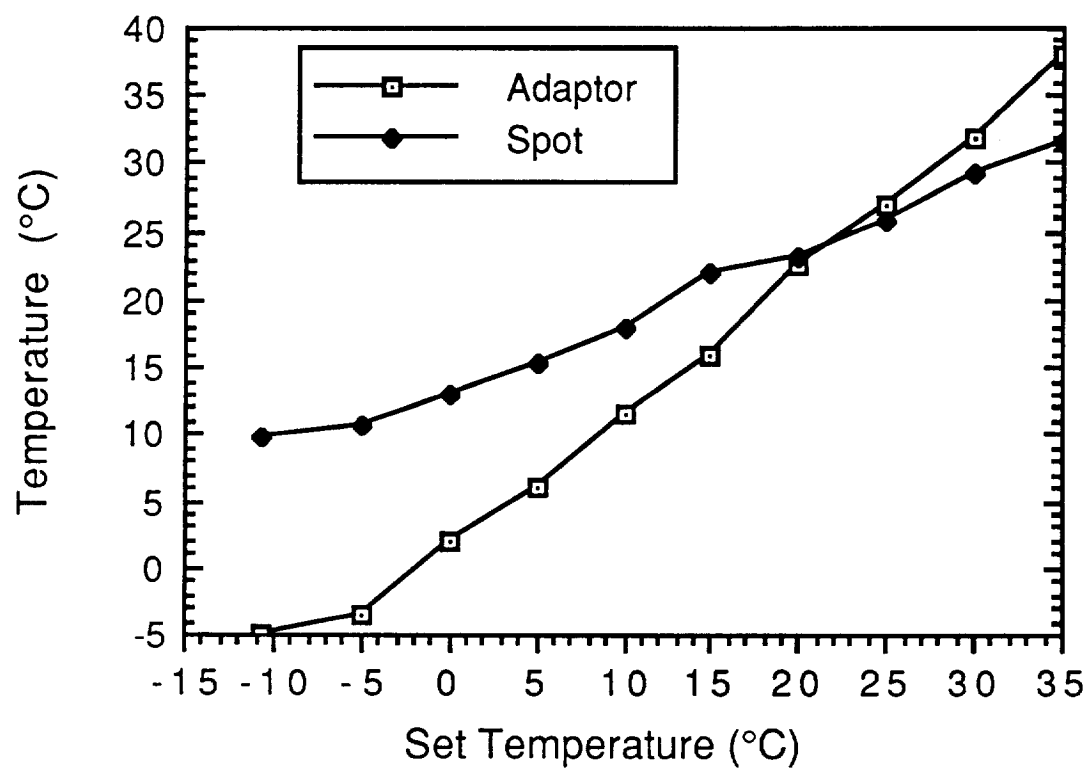
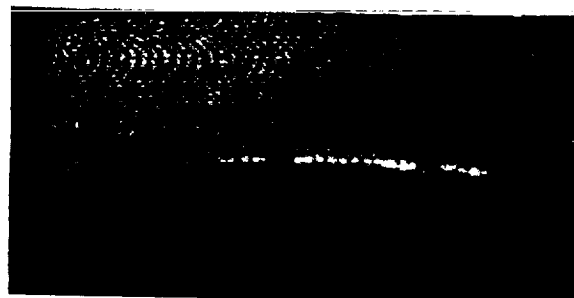


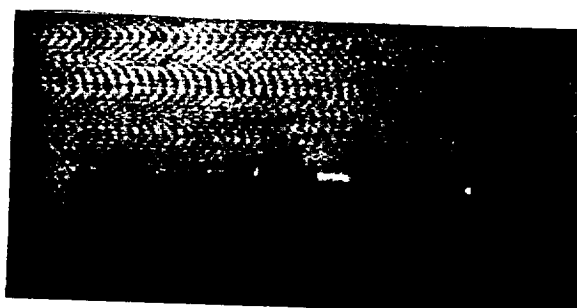
Fig. 15. Temperatures of the adaptor and the cold spot versus set point.



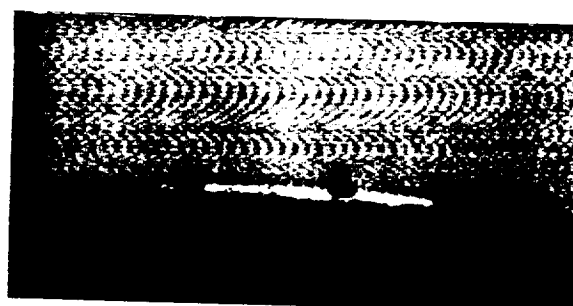
Fig. 16. Ice crystal grown in the Thermonucleator. Ambient temperature was  $10.3^{\circ}\text{C}$ . Probe temperatures were a)  $-6.8^{\circ}\text{C}$  (0.24mm), b)  $-11.5^{\circ}\text{C}$  (0.89mm) and c)  $-13.1^{\circ}\text{C}$  (1.56mm).



a)



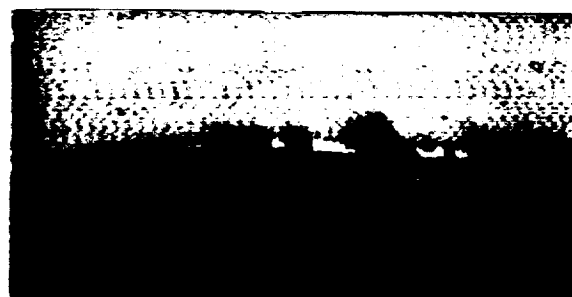
b)



c)



d)



e)

Fig. 17 Lysozyme crystals grown in the Thernonucleator. a) Ambient: 15°C, probe: 10°C; b) ambient: 15°C, probe: -5°C; c) ambient: 22°C, probe: 28°C; d) ambient: 18°C, probe: 15°C and e) ambient: 15°C, probe: 10°C. The crystal sizes were a) 33 $\mu$  (lt) and 22 $\mu$  (rt), b) 55 $\mu$ , 33 $\mu$ , 89 $\mu$  and 167 $\mu$  (lt to rt), c) 22 $\mu$  (lt) and 33 $\mu$  (rt), d) 33 $\mu$  (lt) and 44 $\mu$  (rt), and e) 89 $\mu$ , 44 $\mu$  and 89 $\mu$  (lt to rt).

growth had occurred (fig. 17b). The temperatures were raised ( ambient: 22°C, probe: 28°C) to redissolve the crystals. After 22 hours, only two crystals remained (fig. 17c) and these were located at the positions of the original two crystals. The temperatures were again lowered to increase the supersaturation to 0.8. Over 2 days, the crystals increased in lateral dimension by approximately 10 $\mu$  (fig. 17d). Increasing the supersaturation to 3.0 increased the growth rate but also induced secondary nucleation ( fig. 17e). The original crystals had approximately doubled in linear dimension at the end of the experiment (98 hours of regrowth).

## CONCLUSIONS

The redesign of the Thermonucleator produced an apparatus that was considerably reduced in size and more amenable to use in a  $\mu$ g environment. The individual unit requires only outside connections to a source of cooling fluid (water or a similar liquid) and to two temperature controllers. The use of thermoelectric elements eliminated the need for the liquid nitrogen cooling that was used in the original design. The reduced size will allow several units to be mounted in a small space.

The behavior of the new Thermonucleator closely duplicates that of the original design. The formation and shape of the ice crystals showed that the temperature distribution in the new apparatus closely approximates that of the old one which was as expected. The lysozyme crystallization duplicated that which was done in the old Thermonucleator. The control of the dissolution and regrowth of the crystals was easier due to the more direct control of both the ambient and spot temperatures.

The thermoelectric based unit will require more development before it is ready for use in a  $\mu$ g environment.

## SUMMARY

The goals of this research program were to use Atomic Force Microscopy (AFM) to study the growth of and defects in protein crystal, and to design and evaluate a Thermonucleator more suited to a  $\mu$ g environment and multiple unit operation.

The AFM studies confirmed that protein crystals do grow by a step spreading mechanism. The observed step height for growth on a 110 face of tetragonal lysozyme corresponded closely with the lattice dimension along the 110 direction. Some step bunching was observed, but it was not excessive in the samples we studied. The source of the steps was not found.

The AFM revealed two types of defects. One was a localized retardation of step propagation along 0.2 to 0.3 $\mu$  of the step length. The second was the formation of pits in the growth facet. The causes for these defects were not observed.

These results do not represent the limits of what can be observed with AFM. However, AFM should be combined with other microscopy techniques to pin point areas to be studied rather

than trying to search the whole surface area of the crystal. The AFM studies should also be combined with growth rate studies to obtain a more complete picture of the crystal growth and defect generation mechanisms and their relationship to growth conditions.

A new Thermonucleator based on thermoelectric technology was designed and constructed. The new apparatus was much more compact than the original unit and required connection to only a cooling fluid and two temperature controllers. Its performance was essentially the same as that of the original Thermonucleator.

The new apparatus requires more development before it will be ready for either general laboratory use or use in  $\mu\text{g}$ . Some form of nucleation detection should be incorporated to eliminate the need for redissolving unwanted crystals before continuing the crystal growth. The incorporation of a light scattering nucleation detector should be facilitated by the localization of nucleation provided by the cold probe.

## REFERENCES

1. L. DeLucas, private communication.
2. W. Fowles, L. DeLucas, P. Twigg, S. Howard, E. Meehan, and J. K. Baird, *J. Crystal Growth* 90, 117 (1988).
3. L. Sibille, J. C. Clunie and J. K. Baird, *J. Crystal Growth*, 110, 80 (1991).
4. L. Sibille and J. K. Baird, *J. Crystal Growth*, 110 72 (1991).
5. M. Pusey, private communication.
6. E. Cacioppo, private communication
7. E. Cacioppo, S. Munson, and M. L. Pusey, *J. Crystal Growth* , 110,(1991) 66 and, E. Cacioppo and M. L. Pusey, submitted to *J. Crystal Growth*.
8. A. McPherson, Preparation and Analysis of Protein Crystals (John Wiley & Sons, New York, 1982) Chap. 4, p. 128
9. B. W. Matthews, *J. Mol. Biol.* 33 (1968) 499.
10. NASA Tech Briefs, 15 (9) (1991) 106.
11. B. Gebhart, Y. Jaluria, R. L. Mahajan, and B. Sammakia, Buoyancy Induced Flows and Transport (Hemisphere Publishing Corp., New York, 1988) Appendix F, p 946.
12. G. Homsy. private communication.
13. S. D. Durbin and W. E. Carlson, *J. Crystal Growth* 122 71 (1992)